Inorganica Chimica Acta 401 (2013) 85–94

Contents lists available at SciVerse ScienceDirect

Inorganica Chimica Acta

journal homepage: www.elsevier.com/locate/ica

Oligonuclear homo- and mixed-valence manganese complexes based on thiophene- or aryl-carboxylate ligation: Synthesis, characterization and magnetic studies

Reda F.M. Elshaarawy [a,c], Yanhua Lan [b,*], Christoph Janiak [c,*]

[a] Faculty of Science, Suez Canal University, Suez, Egypt
[b] Institute of Inorganic Chemistry, Karlsruhe Institute of Technology, Engesserstrasse 15, 76131 Karlsruhe, Germany
[c] Institut für Anorganische Chemie und Strukturchemie, Heinrich-Heine Universität Düsseldorf, 40204 Düsseldorf, Germany

ARTICLE INFO

Article history:
Received 1 November 2012
Received in revised form 5 March 2013
Accepted 8 March 2013
Available online 24 March 2013

Keywords:
Manganese
Thiophenecarboxylate
Cluster
Magnetism
Mixed-valence
Butterfly core

ABSTRACT

Mixed-valence trinuclear manganese compounds $[Mn_3O(O_2CTh)_6(L)_x(H_2O)_y]\cdot n(solvent)$ (Th = thiophene, **1**·CH_3CN: L = pyridine (py), $x = 3$, $y = 0$, $n = 1$, solvent = CH_3CN; **1**·∼H_2O: L = py, $x = 3$, $y = 0$, $n = \sim 1$, solvent = H_2O; **2**: L = py, $x = 2$, $y = 1$, $n = 0.25$, solvent = CH_3CN; **3**: L = 3-Mepy, $x = 2$, $y = 1$, $n = 0$) containing a $[Mn^{II}Mn_2{}^{III}(\mu_3\text{-}O)]^{6+}$ core have been prepared. Homo-valence tetranuclear manganese complexes $(NBu^n{}_4)[Mn_4O_2(O_2CAr)_9(L)]$ (**4**·$ThCO_2H\cdot CH_2Cl_2$: Ar = –Th, L = EtOH; **6**: Ar = –Ph, L = H_2O; **7**: Ar = –Ph-*p*-Me, L = H_2O; **8**·CH_2Cl_2: –Ph-3,5-Me_2, no L) with a $[Mn^{III}{}_4(\mu_3\text{-}O)_2]^{8+}$ core and $[Mn^{II}Mn^{III}{}_3O_2(O_2CTh)_7(bpy)_2]$ (**5**) were synthesized, structurally and magnetically characterized. Compounds **1**–**3** were obtained by comproportionation of $Mn^{II}(O_2CMe)_2\cdot 4H_2O$ with $(NBu^n{}_4)Mn^{VII}O_4$ in aprotic pyridine (**1**) or aprotic/protic py/EtOH (**2**) or Mepy/EtOH (**3**) solvent mixtures. Clusters **4**–**8** were synthesized by comproportionation of $Mn^{II}(O_2CAr)_2\cdot xH_2O$/ArCOOH with $(NBu^n{}_4)Mn^{VII}O_4$ in EtOH/CH_3CN. X-ray structural characterization of the 2-thiophenecarboxylate ($ThCO_2^-$) containing compounds **1**·CH_3CN, **1**·∼$2H_2O$ and **4**·$ThCO_2H\cdot CH_2Cl_2$ revealed a thiophene ring disorder about the $(O_2)C$–C(Th) bond so that the S atom and opposite (**5**–)CH group are distributed over two ring positions each. The Mn^{II} atom in the approximately isosceles triangular $[Mn^{II}Mn_2{}^{III}(\mu_3\text{-}O)]^{6+}$ cores in **1** could be clearly assigned from bond valence sum calculations and bond distances. The $[Mn_4(\mu_3\text{-}O)_2]^{8+}$ core in the anionic complexes in the structures of **4**·$ThCO_2H\cdot CH_2Cl_2$ and **8**·CH_2Cl_2 has an all Mn^{III} oxidation level and "butterfly-like" arrangement. The magnetic properties of **4**–**8** were investigated by variable temperature magnetic susceptibility and magnetization measurements. Similar magnetic behavior was observed for the $[Mn^{III}{}_4(\mu_3\text{-}O)_2]^{8+}$ butterfly-core compounds **4**, **6**–**8**, with antiferromagnetic interactions between pairs of manganese ions with amplitude of $\sim 14.5\ cm^{-1}$ and $\sim 4.6\ cm^{-1}$ for the $Mn_b\cdots Mn_b$ and $Mn_b\cdots Mn_w$ coupling, respectively (b = body, w = wing). Changing the Ar-ligand size in $[Mn_4O_2(O_2CAr)_9(L)]^-$ does not have a significant effect on the magnetic properties of these butterfly clusters.

1. Introduction

The synthesis of oligonuclear manganese clusters (Mn_{3-9}) has been stimulated by their biological role and magnetochemistry. Manganese is prominent in the active sites of many metallobiomolecules [1], and the interest is, for example, to obtain molecules that can mimic the oxygen-evolving center (OEC) of photosystem II (PSII) or photosynthetic water oxidation center (WOC) which is responsible for the photosynthesis process in the green plants and cyanobacteria [2–4]. Mn clusters possess considerable high-spin (S) ground states values with a large zero-field splitting parameter (D) (compared to other 3d transition-metal clusters) which appears to be a consequence of the presence within the Mn_x aggregate of (i) ferromagnetic exchange interactions between at least two of the Mn centers [5] and/or (ii) spin frustration effects (when $x \geqslant 3$ and Mn_x alignment in certain direction) [6,7] and (iii) Jahn–Teller distorted d^4-Mn^{3+} ions. Hence, such Mn_x clusters function as nanoscale magnets below their critical temperature [8]. Such Single-Molecule Magnets (SMMs) do not only display magnetization hysteresis, but also quantum tunneling of magnetization (QTM) [9] and quantum phase interference (QPI), [10] and as such they are promising new materials for data storage and quantum computing.

Oxido-centered mixed-valence trinuclear systems containing a $[Mn^{II}Mn_2{}^{III}(\mu_3\text{-}O)]^{6+}$ core and homo-valence tetranuclear manganese

* Corresponding authors. Tel.: +49 2118112286.
E-mail addresses: reda_elshaarawi@science.suez.edu.eg, Reda.El-Shaarawy@uni-duesseldorf.de (R.F.M. Elshaarawy), yanhua.lan@kit.edu (Y. Lan), janiak@uni-duesseldorf.de (C. Janiak).

0020-1693/$ - see front matter © 2013 Elsevier B.V. All rights reserved.
http://dx.doi.org/10.1016/j.ica.2013.03.019

complexes with a $[Mn^{III}_4(\mu_3\text{-}O)_2]^{8+}$ core receive remarkable attention. $[Mn_3O(O_2CR)_6L_3]^{n+}$ (n = 0, 1; L = pyridine, H_2O) with either a $[Mn^{II}Mn^{III}_2(\mu_3\text{-}O)]^{6+}$ or a $[Mn^{III}_3(\mu_3\text{-}O)]^{7+}$ [2–4,11] core are good starting materials for synthesizing manganese polynuclear complexes [12] and is valued for systematic studies of metal–metal interactions in clusters. However, these trinuclear systems are antiferromagnetically coupled with small S values, and, therefore, they are not SMMs [6,11,13]. A $[Mn_4(\mu_3\text{-}O)_2]$ core can either have a "butterfly" or a planar arrangement of the metal atoms (Fig. 1a) with three possible oxidation levels for the metal centers: $Mn^{II}_2Mn^{III}_2$ as in $[Mn_4O_2(O_2CMe)_6(bpy)_2]$ [6,13] (bpy = 2,2′-bipyridine), $Mn^{II}Mn^{III}_3$ as in $[Mn_4O_2(O_2CPh)_7(bpy)_2]$ [14], Mn^{III}_4 as in $(NBu^n_4)[Mn_4O_2(O_2CPh)_9(H_2O)]$ [14] and $[Mn_4O_2(O_2CR)_7(L)_2]^-$ (L = picolinate, 8-hydroxyquinolinate, 2-(oxymethyl)-pyridine anion and dibenzoylmethanate anion) [3,15]. As a result of the spin-state for Mn-ions (Mn^{II} = d^5, $S = {}^5/_2$; Mn^{III} = d^4, S = 2), the probable ground-state spin (S_T) due to spin-frustration phenomena are ${}^7/_2$, ${}^5/_2$ and 3, respectively (Fig. 1b) [16,17].

One important goal in this area of research is not just to construct new examples of high-spin molecules and SMMs, but also to build up families of related compounds so that structure–magnetization relations can be investigated. In this endeavor, two successful but opposing strategies have been employed: the first is the use of rigid bridging ligands that impose the geometry on the resultant cluster [18], and the second is the use of flexible ligands that impose little or no geometrical constraints [19]. Another aim of our research program is to design and build new oligonuclear Mn clusters with sulfur-containing capping ligands which are possible surface-binding candidates (due to presence of free sulfur donor sites, not coordinated to Mn atoms) together with an SMM behavior.

Carboxylate ligands such as 2-thiophenecarboxylate (–OC_2Th) have previously been used in the synthesis of $[Mn(OC_2Th)(2,2'\text{-bpy})_2](ClO_4)_2$ [20] but rarely in the synthesis of paramagnetic oligonuclear Mn clusters such as $[Mn_{12}O_{12}(OC_2Th)_{16}(H_2O)_4]$ [21].

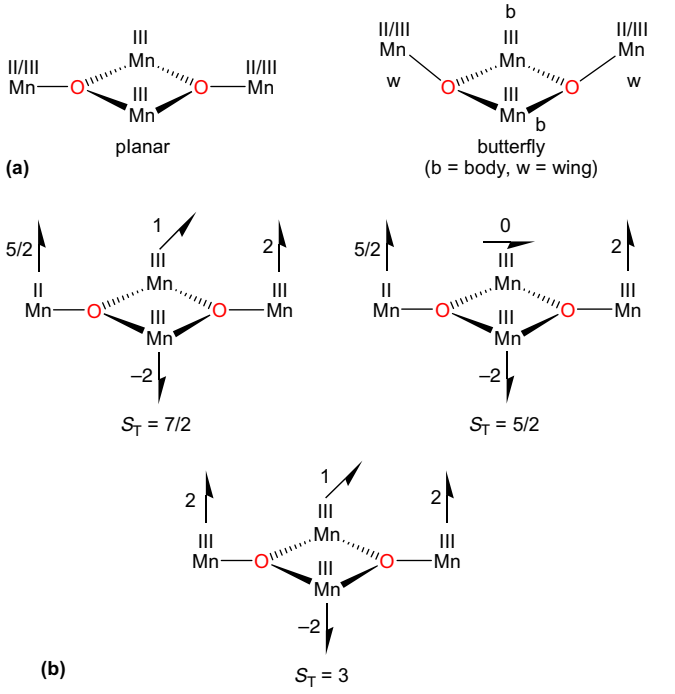

Fig. 1. (a) Possible Mn arrangements and (b) probable ground-state spin (S_T) of $[Mn_4(\mu_3\text{-}O)_2]$ cores.

A noticeable feature in thiophenecarboxylato-metal chemistry is that, except for few examples [22], the thiophene ring (Th) is disordered about the (O_2)C–C(Th) bond and adopt one of two preferred orientations such that the S atom and opposite (**5**–)CH group are distributed over two ring sites (Fig. 2) [23].

We have recently initiated a study of oligo-manganese magnetic systems with simultaneous pyridine (py) or 3-methylpyridine (3-Mepy), water and 2-thiophenecarboxylate ($^-O_2$CTh), benzoate ($^-O_2$CPh), p-methylbenzoate ($^-O_2$CPh-p-Me) or 3,5-dimethylbenzoate ($^-O_2$CPh-3,5-Me_2) bridges. Here we report four new Mn_3 clusters with sulfur-capping 2-thiophenecarboxylate ligands of general formula $[Mn_3O(O_2CTh)_6(L)_x(H_2O)_y].n$(solvent) (**1**·$CH_3CN$: L = py, x = 3, y = 0, n = 1, solvent = CH_3CN; **1**·∼H_2O: L = py, x = 3, y = 0, n = ∼1, solvent = H_2O; **2**: L = py, x = 2, y = 1, n = 0.25, solvent = CH_3CN; **3**: L = 3-Mepy, x = 2, y = 1, n = 0). Also the syntheses, structure and magnetochemical characterization of novel butterfly-like complexes $(NBu^n_4)[Mn_4O_2(O_2CTh)_9(L)]$ (**4**·$ThCO_2H$·CH_2Cl_2: Ar = -Th, L = EtOH; **6**: Ar = -Ph, L = H_2O; **7**: Ar = -Ph-p-Me, L = H_2O; **8**·CH_2Cl_2: –Ph-3,5-Me_2, no L), and $[Mn_4O_2(O_2CTh)_7(bpy)_2]$ (**5**) are the subject of this paper. The magnetic susceptibilities of these new tetranuclear complexes (**4**–**8**) at various temperatures were described in order to establish the magneto-structural relationship.

2. Experimental

2.1. Physical measurements

Elemental analyses (EA) were determined on a Vario EL instrument from Elementaranalysensysteme GmbH. Manganese analyses were carried out by atomic absorption spectrometry on a Vario-6 AAS from Analytik Jena. FT-IR spectra were recorded on a Bruker Tensor-37 FT-IR spectrophotometer in the range 400–4000 cm^{-1} as KBr discs or in the 4000–550 cm^{-1} region with 2 cm^{-1} resolution with an ATR unit (Platinum ATR-QL, Diamond). UV/Vis spectra were measured at 25 °C in dichloromethane (CH_2Cl_2) (10^{-5} M) on a Shimadzu UV-2450 spectrophotometer using quartz cuvettes (1 cm). The magnetic susceptibility measurements were carried out for crystalline samples (**4**–**8**) using a Quantum Design Squid MPMS-XL magnetometer between 1.8 and 400 K for DC applied fields ranging from 0 to 7 T. The magnetic data were corrected by the diamagnetic contribution from the sample holder.

2.2. Materials and syntheses

Unless stated otherwise all chemical reagents and solvents were of analytical grade, purchased commercially, and used as received. Mn(II) salts of benzoate ($Mn(O_2CPh)_2{\cdot}2H_2O$) [14], 3,5-dimethylbenzoate ($Mn(O_2CPh\text{-}3,5\text{-}(Me)_2)$) [24], 2-thiocarboxylate ($Mn(O_2CTh)_2{\cdot}4H_2O$) [25], $(NBu^n_4)NMnO_4$, [11,26] and $(NBu^n_4)[Mn_4O_2(O_2CPh)_9(H_2O)]$ [14] (**6**) were synthesized using reported methods. Mn(II) p-methylbenzoate ($Mn(O_2CPh\text{-}p\text{-}Me)_2{\cdot}2H_2O$) was prepared from manganese(II) chloride tetrahydrate, p-toluic acid, and sodium hydroxide in a 1:2:2 M ratio in aqueous media and

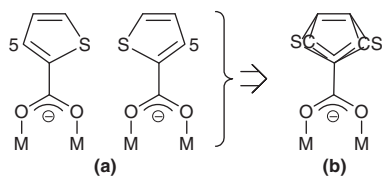

Fig. 2. (a) Typical sulfur atom or thiophene ring disorder in the planar 2-thiophenecarboxylate ligand and (b) graphical representation where the two possible orientations of the thiophene ring are superimposed.

its composition was confirmed by elemental analysis. All manipulations were performed under aerobic conditions.

Caution! Organic permanganates should be handled with extreme caution. Detonations of some organic permanganates have been reported while drying at high temperatures.

cyclo-μ_3-Oxido-tris(pyridine-κ*N*)-hexakis(μ-2-thiophenecarboxylato-κ*O*:*O*′)-manganese(II)–dimanganese(III), $[Mn_3O(O_2CTh)_6(py)_3]$ (1) as acetonitrile solvate or hydrate. The freshly synthesized solid $(NBu^n_4)MnO_4$ (1.14 g, 3.15 mmol) was added portion-wise (over 15 min) to a magnetically stirred solution of $Mn(O_2CMe)_2{\cdot}4H_2O$ (1.00 g, 4.075 mmol) and $ThCO_2H$ (3.93 g, 30.8 mmol) in pyridine (10 mL, 124 mmol) to give a dark brown homogeneous solution. After complete addition stirring was continued for another 15 min and then the solvent was removed in *vacuo* to give a brown oil residue. This residue was extracted with EtOH (50 mL) to give a reddish-brown solution and left the undissolved brown solid that was separated by filtration. The EtOH filtrate was discarded. The brown solid residue was extracted into a minimum amount of CH_3CN and filtered, then the filtrate was allowed to concentrate by slow evaporation to give dark brown crystals of $1{\cdot}CH_3CN$ which was collected by filtration and dried in *vacuo*. Yield of $1{\cdot}CH_3CN$ 22% (based on Mn). These crystals could be further re-crystallized via over-layering of their methylene chloride solution with n-hexane/Et_2O solvent mixture to afford crystals of **1** with (an) ill-defined solvent molecule(s), most likely $1{\cdot}{\sim}H_2O$.

Acetonitrile solvate, *Anal.* Calc. for $\mathbf{1}{\cdot}CH_3CN$: $C_{45}H_{33}Mn_3N_3O_{13}S_6{\cdot}CH_3CN$ (1222.98): C, 46.19; H, 2.97; N, 4.58; S, 15.74. Found: C, 45.79; H, 2.91; N, 4.49; S, 15.51%. FT-IR (KBr, cm^{-1}): 3435 (m, br), 1598 (s, sh), 1526 (s, sh), 1424 (s, sh), 1385 (s, sh), 1343 (m, sh), 1120 (m, sh), 1045 (m, sh), 858 (s, sh), 770 (m, sh), 691 (m, sh), 654 (m, sh) and 442 (m, sh).

Hydrate, *Anal.* Calc. for $\mathbf{1}{\cdot}{\sim}H_2O$: $C_{45}H_{33}Mn_3N_3O_{13}S_6{\cdot}H_2O$ (1198.99): C, 45.08; H, 2.94; N, 3.50; S, 16.05; *Anal.* Calc. for $C_{45}H_{33}Mn_3N_3O_{13}S_6{\cdot}2H_2O$ (1217.01): C, 44.41; H, 3.06; N, 3.45; S, 15.81. Found: C, 44.09; H, 2.74; N, 2.88; S, 15.58%. Note that the crystal structure of a single crystal of this compound suggested formulation as a monohydrate. FT-IR (KBr, cm^{-1}): 3432 (m, br), 1601 (s, sh), 1525 (s, sh), 1421 (s, sh), 1385 (s, sh), 1338 (m, sh), 1117 (m, sh), 1043 (m, sh), 858 (s, sh), 770 (m, sh), 690 (m, sh), 658 (m, sh) and 445 (m, sh).

$[Mn_3O(O_2CTh)_6(py)_2(H_2O)]$ (2). $Mn(O_2CMe)_2{\cdot}4H_2O$ (1.00 g, 4.075 mmol) and $ThCO_2H$ (3.93 g, 30.8 mmol) were dissolved in a mixture of pyridine (1.5 mL) and absolute EtOH (10 mL). Then freshly prepared solid $(NBu^n_4)MnO_4$ (0.57 g, 1.575 mmol) was added in small portions with continuous stirring to give a brown homogeneous solution. After 24 h, the resulting grey-green precipitate was separated by filtration, washed with EtOH, and dried in *vacuo* (crude yield > 95%). Recrystallization was accomplished either by slow evaporation of a CH_3CN solution to give deep-green crystals of $\mathbf{2}.0.25CH_3CN$, which were collected by filtration, washed with EtOH, and dried in *vacuo* or by overlayering the solution of **2** in CH_2Cl_2 with hexane to give small microcrystals of $\mathbf{2}.0.5CH_2Cl_2$ after several days which were filtered off and dried in *vacuo*. Yield 58% based on Mn. *Anal.* Calc. for $\mathbf{2}.0.25CH_3CN$, $C_{40.5}H_{30.75}Mn_3N_{2.25}O_{14}S_6$ (1130.14): C, 43.04; H, 2.74; N, 2.79; S, 17.02. Found: C, 43.52; H, 2.74; N, 2.54; S 17.43%. *Anal.* Calc. for $\mathbf{2}.0.5CH_2Cl_2$, $C_{40.5}H_{31}ClMn_3N_2O_{14}S_6$ (1162.34): C, 41.85; H, 2.69; N, 2.41; S, 16.55. Found: C, 42.13; H, 2.80; N, 2.75; S, 16.77%. Other analyses were identical for both solvates. FT-IR (KBr, cm^{-1}): 3392 (m, br), 1597 (s, sh), 1525 (s, sh), 1423 (s, sh), 1385 (s, sh), 1344 (m, sh), 1122 (m, sh), 1045 (m, sh), 859 (s, sh), 769 (m, sh), 694 (m, sh), 655 (m, sh) and 444 (m, sh).

$[Mn_3O(O_2CTh)_6(3\text{-}Mepy)_2(H_2O)]$ (3). This complex was prepared in the same manner as **2**, using 3-methylpyridine instead of pyridine. The isolated solid was filtered off, washed with cold ethanol, ether and then dried in *vacuo*. Crystallization was achieved by slow diffusion of *n*-hexane into the solution of the isolated solid in CH_2Cl_2 for several days. Small crystals obtained were filtered off and dried in *vacuo*. Yield 69% based on Mn of complex **3**. *Anal*. Calc. for $C_{42}H_{34}Mn_3N_2O_{14}S_6$ (1147.93): C, 43.94; H, 2.99; N, 2.44; S, 16.76. Found: C, 44.09; H, 2.69; N, 2.45; S, 16.66%. FT-IR data (KBr, cm^{-1}): 3422 (m, br), 1600 (s, sh), 1525 (m, sh), 1424 (s, sh), 1387 (s, sh), 1340 (m, sh), 1124 (m, sh), 1034 (m, sh), 899 (m, sh), 858 (s, sh), 770 (m, sh), 698 (m, sh), 656 (m, sh) and 444 (m, sh).

(Tetra-n-butylammonium)-[(ethanol-κ*O*)(μ_3-dioxido)hepta-kis(μ-2-thiophenecarboxylato-κ*O*:*O*′)(2-thiophenecarboxylato-κ*O*,*O*′)(2-thiophenecarboxylato-κ*O*)tetramanganate(III)] (2-thiophenecarboxylic acid) dichloromethane solvate, $(NBu^n_4)[Mn_4O_2(O_2CTh)_9(EtOH)]{\cdot}ThCO_2H{\cdot}CH_2Cl_2$ ($\mathbf{4}{\cdot}ThCO_2H{\cdot}CH_2Cl_2$). Freshly-prepared $(NBu^n_4)MnO_4$ (0.45 g, 1.25 mmol) was added portion-wise (over 15 min) to a stirred solution of $Mn(O_2CTh)_2{\cdot}4H_2O$ (1.54 g, 4.05 mmol) and $ThCO_2H$ (3.93 g, 30.7 mmol) in $EtOH/CH_3CN$ (20:10 mL). The resulting reddish brown solution was evaporated under reduced pressure to dryness and then the residue re-dissolved in CH_2Cl_2 (15 mL) to give a dark-red solution. This solution was filtered through Celite, and then layered with a mixture of Et_2O (25 mL) and hexanes (25 mL). After several days, red-brown crystals of $\mathbf{4}{\cdot}ThCO_2H{\cdot}0.5\ CH_2Cl_2$ were formed; they were collected by filtration, washed with Et_2O, and dried in air. The yield based on total available Mn was 63%. *Anal.* Calc. for $C_{68}H_{73}Mn_4NO_{23}S_{10}{\cdot}CH_2Cl_2$ (1897.56): C, 43.76; H, 3.98; Mn, 11.58; N, 0.74; S, 16.90; *Anal.* Calc. for $C_{68}H_{73}Mn_4NO_{23}S_{10}$ (without CH_2Cl_2) (1812.73): C, 45.06; H, 4.06; Mn, 12.12; N, 0.77; S, 17.69. Found: C, 44.02; H, 4.42; Mn, 12.38; N, 0.84; S, 17.34%. FT-IR data (KBr, cm^{-1}): 3431 (m, br), 1704 (w, sh), 1586 (s, sh), 1525 (m, sh), 1422 (s, sh), 1385 (s, sh), 1340 (m, sh), 1126 (m, sh), 1031 (m, sh), 859 (s, sh), 769 (m, sh), 652 (s, sh), 512 (m, sh) and 444 (m, sh).

$[Mn_4O_2(O_2CTh)_7(bpy)_2]$ (5). Method A. A red-brown solution of complex **4** (25 mmol) in THF (20 mL) was overlayered with a solution of bpy (0.080 g, 0.50 mmol) in CH_3CN (20 mL). After 2 days, a dark red-brown crystalline product was isolated by filtration, washed with Et_2O and dried in air; yield 68%. Recrystallization was effective from CH_2C1_2/*n*-hexane to give large black plates which, however, were repeatedly shown to be of poor quality for single-crystal X-ray diffraction. *Anal.* Calc. for $C_{55}H_{37}Mn_4N_4O_{16}S_7$ (1454.13) without potential solvent: C, 45.43; H, 2.56; N, 3.85; S, 15.44. Found: C, 45.58; H, 2.62; N, 3.82; S, 15.88%. Selected IR data (ATR, cm^{-1}): 1698 (m, sh), 1570 (s, sh), 1351 (m, sh), 1265 (w, sh), 1160 (m, sh), 1140 (w, sh), 1088 (m, sh), 1031 (m, sh), 858 (s, sh), 832 (m, sh), 763 (m, sh), 672 (s, sh), 642 (m, sh) and 464 (m, sh).

Method B. To a stirred green–brown solution of $\mathbf{2}{\cdot}0.25CH_3CN$ (0.569 g, 0.5 mmol) in CH_3CN (15 mL) was added solid bpy (0.25 g, 1.6 mmol). The resulting brown solution began to precipitate brown microcrystals of **5** within minutes. After 1 h, the solid was collected by filtration, washed with cold CH_3CN and dried; yield 60–70%. The compound had an identical IR spectrum with the material prepared by method A.

$(NBu^n_4)[Mn_4O_2(O_2CPh)_9(H_2O)]$ (6) was synthesized using a reported method [14] and isolated as reddish-black needle crystals, washed with Et_2O and dried in air; yield 92%. Recrystallization was effective from CH_2Cl_2 by overlayering with Et_2O/*n*-hexane mixture (1:1). *Anal.* Calc. for $C_{79}H_{83}Mn_4NO_{21}$ (1602.27) without potential solvent: C, 59.22; H, 6.22; N, 0.87. Found: C, 59.18; H, 5.22; N, 0.76%. Their IR spectrum is identical with that of authentic complex **4** [14].

$(NBu^n_4)[Mn_4O_2(O_2CPh\text{-}4\text{-}Me)_9(H_2O)]$ (7). This complex was prepared analogous to complex **4** with $Mn(O_2CPh\text{-}p\text{-}Me)_2{\cdot}2H_2O$ and *p*-$MePhCO_2H$ being used as a source of Mn^{II}-ions and 4-methylbenzoate ligation groups. Higher quality X-ray crystals were obtained from the formed solid by re-dissolving it in CH_2Cl_2 (15 mL), filtering the reddish-brown solution through Celite then layering

the filtrate with 2:1 Et_2O/*n*-hexane mixture (30 mL). After several days, red-brown crystals of **7**·0.5 CH_2Cl_2 were formed; they were collected by filtration, washed with Et_2O, and dried in air. Yield 83%. *Anal.* Calc. $C_{88.5}H_{101}ClMn_4NO_{21}$ (1770.69): C, 60.02; H, 5.81; Mn, 12.41; N, 0.79. Found: C, 60.31; H, 6.08; Mn, 12.62; N, 0.81%. FT-IR data (KBr, cm^{-1}): 3431 (m, br), 1607 (s, sh), 1558 (s, sh), 1404 (s, sh), 1177 (s, sh), 1021 (m, sh), 858 (m, sh), 765 (s, sh), 691 (m, sh), 625 (s, sh), 485 (m, sh) and 445 (m, sh).

(Tetra-*n*-butylammonium)[(μ$_3$-dioxido)heptakis(μ-3,5-dimethylbenzoato-κ*O*:*O*′)bis(3,5-dimethylbenzoato-κ*O*,*O*′)tetramanganate(III)] dichloromethane solvate, (NBu^n_4)[Mn_4O_2(O_2CPh-3,5-Me_2)$_9$]·CH_2Cl_2 (8·CH_2Cl_2). As for complex **7** by using Mn(O_2CPh-3,5-Me_2)$_2$ and 3,5-$(Me)_2PhCO_2H$. The resulting precipitate was dissolved in CH_2Cl_2 (15 mL), filtered through Celite, and then layered with hexane (25 mL). Dark brown–red parallelepiped-like crystals were obtained after 2 days. Yield 58%. *Anal.* Calc. for $C_{97}H_{117}Mn_4NO_{20}$·0.5CH_2Cl_2 (1879.18): C, 62.32; H, 6.33 Mn, 11.69; N, 0.75. *Anal.* Calc. $C_{97}H_{117}Mn_4NO_{20}$ (without CH_2Cl_2) (1836.75): C, 63.43; H, 6.42; Mn, 11.96; N, 0.76. Found: C, 62.51; H, 6.71; Mn, 11.36: N, 0.75%. Note that dichloromethane easily evaporates during sample preparation for elemental analysis. The crystal structure of a single crystal of this compound suggested formulation with a full dichloromethane solvate molecule. FT-IR data (KBr, cm^{-1}): 1581 (s, sh), 1394 (s, sh), 1083 (m, sh), 869 (m, sh), 784 (s, sh), 680 (s, sh), 549 (m, sh) and 486 (m, sh).

2.3. X-ray Crystallography

Suitable single crystals were carefully selected under a polarizing microscope. *Data collection:* Single crystal X-ray data of **1**·CH_3CN, **1**·∼H_2O, **4**·$ThCO_2H$·CH_2Cl_2 and **8**·CH_2Cl_2 were collected on Bruker Apex II CCD (**1**·CH_3CN and **8**) and a Rigaku R-axis Spider image plate detector (**1**·∼H_2O, **4**) diffractometer by using graphite-monochromatic Mo Kα radiation (λ = 0.071073 Å) and ω scan mode. Cell refinement with APEX2 [27], data reduction with SAINT (Bruker) [28] or data collection, cell refinement and data reduction with CrystalClear (Rigaku) [29]. *Structure analysis and refinement:* the structure was solved by direct methods (SHELXS-97) [30]; refinement was done by full-matrix least squares on F^2 using the SHELXL-97 program suite [30]; empirical (multi-scan) absorption correction with SADABS (Bruker) [31] or ABSCOR (Rigaku) [32]. All non-hydrogen positions were refined with anisotropic temperature factors. Hydrogen atoms were positioned geometrically and refined using a riding model (AFIX 43 for aromatic CH, AFIX 13 for aliphatic CH and AFIX 23 for CH_2) with $U_{iso}(H) = 1.2\,U_{eq}(CH)$. For CH_3 AFIX 33, 133 or 137 was used with $U_{iso}(H) = 1.5\,U_{eq}(CH)$. 2-Thiophenecarboxylate containing compounds **1** and **4** suffer from the thiophene ring disorder, depicted in Fig. 2. This thiophene disorder could only partially be resolved and, thus, affected the data set quality. Still, the immediate Mn coordinating bridging carboxylate groups and terminal ligand atoms, hence, the core structure {$Mn_3(O)(O_2C)_6(N)_3$} (in **1**·CH_3CN, **1**·∼H_2O) and {$Mn_4(O)_2(O_2C)_9$(EtOH)} (in **4**·$ThCO_2H$·CH_2Cl_2) could be unequivocally refined. Additional disorder was present in **1**·∼H_2O in the lattice water molecule (large thermal ellipsoids, H atoms not found) and one of its pyridine rings, in **8** in the CH_2Cl_2 solvent molecule (rotated by 90°) and in two cation butyl groups. However, in all four structures the {Mn_3(μ-O)} or {Mn_4(μ-O_2)} cores with their bridging carboxyl, O_2C-groups and coordinating pyridine N-atoms or ethanol O-atom could clearly been refined without any disorder and with good temperature factors. Hence, in the structure discussion we will limit ourselves to the central core. Crystal data and details on the structure refinement are given in Table 1. Graphics were drawn with DIAMOND [33].

3. Results and discussion

3.1. Synthesis

Complexes **1**–**3** represents the first examples of a [$Mn^{II}Mn_2^{III}$(μ_3-O)]$^{6+}$ core with thiophenecarboxylate bridges in addition to pyridine, water or 3-methylpyridine terminal ligands. The three new complexes were prepared following the method described by Vincent et al. for the benzoato analog [11]. Comproportionation of $Mn^{II}(O_2CMe)_2$·$4H_2O$ with the strong oxidizing agent (NBu^n_4)$Mn^{VII}O_4$ in the presence of 2-thiophenecarboxylic acid (ThCOOH),

Table 1
Crystal data and structure refinement for compounds **1**·CH_3CN, **1**·∼H_2O, **4**·$ThCO_2H$·CH_2Cl_2 and **8**·CH_2Cl_2.

Compound	**1**·CH_3CN	**1**·∼H_2O	**4**·$ThCO_2H$·CH_2Cl_2	**8**·CH_2Cl_2
Empirical formula	$C_{47}H_{36}Mn_3N_4O_{13}S_6$	$C_{45}H_{33}Mn_3N_3O_{14}S_6$	$C_{69}H_{75}Cl_2Mn_4NO_{23}S_{10}$	$C_{98}H_{119}Cl_2Mn_4NO_{20}$
M/g mol^{-1}	1221.98	1196.92	1897.56	1921.60
Crystal size (mm)	0.36 × 0.31 × 0.25	0.28 × 0.24 × 0.19	0.40 x 0.20 x 0.08	0.15 × 0.12 × 0.06
Temperature (K)	296(2)	203(2)	203(2)	203(2)
θ range (°) (completeness)	1.63–25.15 (99.1%)	3.00–22.91 (97.8%)	3.00–22.59 (97.8%)	1.46–25.50 (97.9%)
h; *k*; *l* range	±22, ±27, −28, 27	±20, −24, 25, ±25	±15, ±21, −29, 30	±20, −27, 33, ±27
Crystal system	orthorhombic	orthorhombic	monoclinic	monoclinic
Space group	*Pbca*	*Pbca*	$P2_1/c$	$P2_1/c$
a (Å)	19.1258(9)	18.974(4)	14.723(3)	16.5930(13)
b (Å)	23.0759(12)	22.931(5)	20.353(4)	27.958(3)
c (Å)	23.5440(12)	23.640(5)	28.020(6)	22.7744(17)
β (°)	90	90	92.77(3)	108.246(4)
V (Å^3)	10391.0(9)	10 286(4)	8386(3)	10033.9(14)
Z	8	8	4	4
D_{calc} (g/cm^3)	1.562	1.546	1.503	1.272
μ (mm^{-1})	1.025	1.035	0.971	0.610
F(000)	4968	4856	3896	4032
Maximum/minimum transmembrane	0.7836/0.7091	0.8277/0.7604	0.9263/0.6973	0.9643/0.9157
Reflections collected	120394	65041	77460	85556
Independent reflections (R_{int})	9215 (0.2127)	6914 (0.1306)	10836 (0.0854)	18263 (0.0872)
Data/restraints/parameters	9215/0/697	6914/66/692	10836/0/992	18263/0/1157
Maximum/minimum Δρ (e Å^{-3})[a]	0.514/−0.747	1.308/−0.799	0.762/−0.844	0.394/−0.429
R_1/wR_2 [$I > 2(I)$][b]	0.0650/0.1385	0.1016/0.2695	0.0721/0.1976	0.0550/0.1195
R_1/wR_2 (all data)[b]	0.1662/0.1809	0.1718/0.3233	0.1150/0.2280	0.1165/0.1418
Goodness-of-fit on F^2[c]	0.991	1.034	1.042	1.024

[a] Largest difference peak and hole.
[b] $R_1 = [\Sigma(||F_o| - |F_c||)/\Sigma|F_o|]$; $wR_2 = [\Sigma[w(F_o^2 - F_c^2)^2]/\Sigma[w(F_o^2)^2]]^{1/2}$.
[c] Goodness-of-fit = $[\Sigma[w(F_o^2 - F_c^2)^2]/(n-p)]^{1/2}$.

as source for carboxylate bridges, and pyridine (py), aprotic solvent, afforded compound **1** with terminal pyridine ligands only. While in the presence aprotic/protic mixed solvent (Py/EtOH or Mepy/EtOH), compounds **2** and **3** with a terminal water ligand were isolated (Scheme 1). Compounds **1** and **2** crystallize with solvent molecules (CH_3CN, CH_2Cl_2).

The tetranuclear manganese complexes (**4, 6–8**), containing a $[Mn^{III}_4(\mu_3\text{-}O)_2]^{8+}$ core with a "butterfly" deposition of four Mn-atoms, were obtained in a quantitative yield and high purity via the comproportionation reaction of $Mn^{II}(O_2CAr)_2{\cdot}xH_2O$/ArCOOH, as a source of Mn^{II}-ions and carboxylates ligation ligands, and $(NBu^n_4)Mn^{VII}O_4$ in EtOH/CH_3CN (2:1 v/v) solvent mixture under ambient conditions (Scheme 2). Single crystal of **4** and **8** were isolated via over-layering of the CH_2Cl_2 solution with n-C_6H_{14}/Et_2O (1:1 v/v). By charge balance arguments, the four Mn-ions in complex **7** were concluded to be homo-valent (Mn^{III}_4).

Complex **4** is a starting material to a new mixed-valence $Mn^{II}Mn^{III}_3$ cluster, containing both 2,2-bipyridine (bpy) and thiocarboxylate (^-O_2CTh) bridging groups, through a peripheral-ligand substitution. Treatment of complex **4** with 2 equivalents of 2,2-bipyridine (bpy) in THF/CH_3CN (1:1 v/v) afforded $[Mn_4O_2(O_2CTh)_7(bpy)_2]$ (**5**) with a $[Mn^{II}Mn^{III}_3O_2]^{7+}$ core, analogous to $[Mn_4O_2(O_2CPh)_7(bpy)_2]$ [14], rather than the expected $[Mn_4O_2(O_2CTh)_7(bpy)_2](O_2CTh)$ with $[Mn^{III}_4O_2]^{8+}$. This reduction of one Mn-center could be attributed to solvent, solvent impurities or excess ligand, and facilitated by the oxidizing tendency of Mn^{III}. Another pathway to get tetranuclear **5** is from the trinuclear complex, $[Mn_3O(O_2CTh)_6(py)_2(H_2O)]$ **2** by means of bpy, followed by carboxylate substitution. This reaction was studied by Vincent et al. using the analogous compounds $[Mn_3O(O_2CR)_6(py)_2(H_2O)]$ (R = Ph, Ph-3-Me) (Eq. (1)) [11].

$$4/3\,[Mn_3O(O_2CR)_6(py)_2(H_2O)] + 2bpy \rightarrow [Mn_4O_2(O_2CR)_7(bpy)_2] + RCO_2H + 2/3H_2O + 8/3py \quad (1)$$

3.2. Vibration spectra and carboxylate binding modes

The study of the IR spectral data was quite informative in characterizing the coordination mode of the carboxylate ligands to the Mn ions. The diagnostic IR spectral bands with their assignments of the complexes are shown in the Supporting information, Table S1. The carboxylate group can display a wide variety of coordination modes toward metal ions (Fig. S1 in Supporting information), which lead to diverse types of molecular geometries [34]. The IR spectral method has proven to be a suitable technique to give information about the metal-carboxylate binding modes.

IR spectra of complexes **1–3** display characteristic absorption bands for the coordinated ligands in the 1620–1340 cm^{-1} region (Supporting information, Fig. S2) due to different modes of carboxylate binding. Three such carboxylate stretches observed for **1–3** at ~1598, ~1525 and ~1424–1385 cm^{-1} are assigned to the asymmetric and symmetric carboxylate vibrations, respectively. The frequency gaps ($\Delta\nu$) between these bands have an average $\Delta\nu = \nu_a(COO^-) - \nu_s(COO^-)$ of ~157 cm^{-1} which is less than that

$Mn(OAc)_2{\cdot}4H_2O$ + ThCOOH + $(NBu^n_4)MnO_4$

py, RT	$[Mn_3O(O_2CTh)_6(py)_3]$	1
py/EtOH, RT	$[Mn_3O(O_2CTh)_6(py)_2(H_2O)]$	2
Mepy/EtOH, RT	$[Mn_3O(O_2CTh)_6(Mepy)_2(H_2O)]$	3

Scheme 1. Synthesis of trinuclear complexes **1–3** with a mixed-valence $[Mn^{II}Mn^{III}_2(\mu_3\text{-}O)]^{6+}$ core.

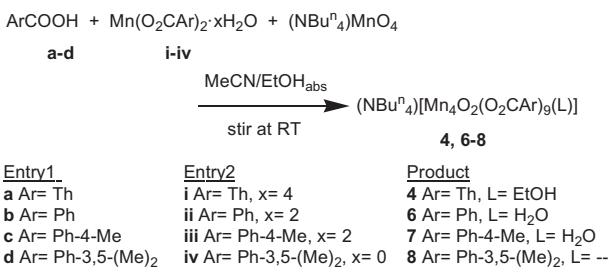

Scheme 2. Synthesis of tetranuclear complexes **4, 6–8** with homo-valence $[Mn^{III}_4(\mu_3\text{-}O)_2]^{8+}$ cores.

for the corresponding NaO_2CTh salts (Supporting information, Table S2). This $\Delta\nu$ value reveals that (i) the carboxylate ligation is in the bidentate bridging mode ($\mu_{1,3}$- or $\eta^1{:}\eta^1{:}\mu_2$-) [35,36] and (ii) these trinuclear exhibit two types of carboxylate bridges, one which connects two mixed-valence manganese centers (Mn^{II} and Mn^{III}) while the other connects two isovalent manganese(III) centers and all in a $\eta^1{:}\eta^1{:}\mu_2$-*syn,syn* modes (cf. Fig. 3).

The band at ca. 1340 cm^{-1} is attributed to the ν(CSC/thiophene) stretch [22]. Bands between 440 and 800 cm^{-1} are assigned to the asymmetric in-plane vibration of the Mn_3O core. The reduction in site symmetry from D_{3h}, for $(Mn^{III})_3O$ trinuclear complexes to C_{2v} in $(Mn^{III}_2Mn^{II})O$ compounds, **1–3** lifts the degeneracy of the asymmetric in-plane stretches of the Mn_3O core to give two bands [37]. Shoulders around 1525 and 1199 cm^{-1} are attributed to the py and Mepy vibrations. Additionally, two moderate intense bands at 859 and 800 cm^{-1} are assigned to py ligands [38].

Sections of the IR spectra for the tetranuclear compounds **6–8** are presented in the Supporting information (Fig. S3). The separation between $\nu_a(COO^-)$ and $\nu_s(COO^-)$ for these compounds is significantly less than for the carboxylate anion in $NaO_2CAr{\cdot}xH_2O$ (cf. Table S2) which is as expected for the bidentate bridging mode in **4–8**. However, the frequency difference between the asymmetric and symmetric carboxylate vibrations of 153 cm^{-1} for the tetranuclear complexes **4** and **5** (with the $[Mn^{III}_4(\mu_3\text{-}O)_2]^{8+}$ core) is slightly lower than for the trinuclear complexes **1–3** (with the $[Mn^{II}Mn^{III}_2(\mu_3\text{-}O)]^{6+}$ core). This suggests that, the energy difference between $\nu_a(COO^-)$ and $\nu_s(COO^-)$ decreases upon oxidation of Mn^{II} to Mn^{III}. Additionally, complex **4** showed another asymmetric/symmetric vibrational shift difference of $\Delta\nu$ = 246 cm^{-1}, which is consistent with a monodentate coordination mode (η^1) of carboxylate ligation [22], hence compound **4** contains mixed-(monodentate/bidentate) carboxylate bridges (cf. Fig. 4a). The $\Delta\nu$ value of 187 cm^{-1} for complex **8** is consistent with the bidentate and chelating modes (cf. Fig. 4b).

Additionally, the presence of the coordinated H_2O molecules in all complexes is manifested by a medium intense broad IR band of at ~3430 cm^{-1} with a stretch at ca. 859 cm^{-1}, which are assigned to νOH and ρ_rOH vibrations [35]. Moreover, the moderate intense band at ca. 680 and several weaker bands observed in the 510–425 cm^{-1} range are characteristic for ν(Mn–O) of the Mn_4O_2 core [39].

3.3. Electronic absorption spectra

The electronic spectra (ES) of the trinuclear complexes **1–3** exhibit similar features, where all display a shoulder and two intense absorption peaks at *ca.* 206, 220 and 245 nm which are assigned to the intra- and inter-thiophenecarboxylate charge transfer ($\pi \rightarrow \pi^*$, LLCT), respectively [23]. Another features of these spectra are a maximum at ~264 nm and a broad shoulder at ca. 280 nm. The maximum is assignable to a difference in enhancement of pyridine $\pi \rightarrow \pi^*$ transitions [40]. The origin of the broad shoulder was

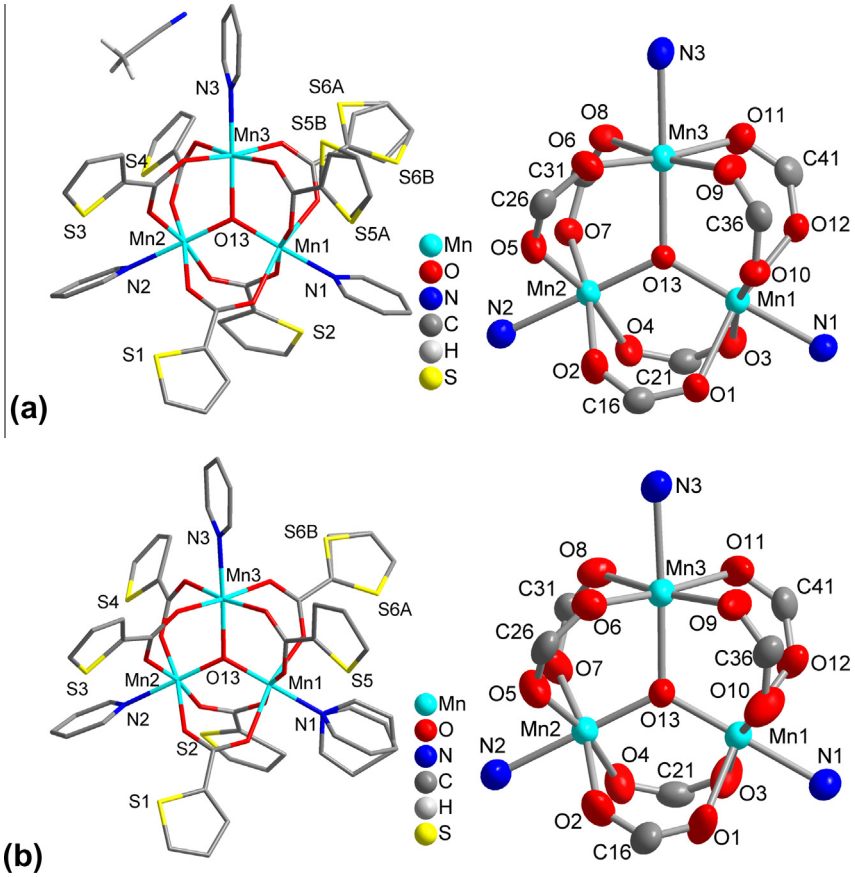

Fig. 3. Wire-frame and ellipsoid-core model (50% probability) of complex **1** in (a) **1**·CH_3CN and (b) **1**·~H_2O. Note the resolved thiophene and pyridine disorder. H atoms are not shown for clarity. In (b) the oxygen atom of the water molecule is not shown. Both complexes employ the same atom numbering scheme for direct comparison of their bond lengths (cf. Table 2). The Mn(II) atom is labeled as Mn3 and points upwards.

deduced via studying the effect of ligand substitution in the UV/Vis spectra of the trinuclear complexes **1**–**3.** Their spectra display only a slight shift in the energy of pyridine-based $\pi \rightarrow \pi^*$ transitions which suggests that this shoulder may arise from a high-energy pyridine-to-Mn(III) charge transfer band which is relatively insensitive to methylation of the pyridine in the 3-position, consistent with the previously revealed electronic spectral features accompanying the pyridine ligands substitution with imidazole (ImH) (i.e. $[Mn_3O(O_2CMe)_6(py)_3]ClO_4$ and $[Mn_3O(O_2CMe)_6(ImH)_3](O_2CCH_3)$ [2,11]. Additionally, the lower energy spectral bands at ~315 and ~490 nm are attributed to ligand-to-Mn(III) charge transfer transitions (MLCT/LMCT) involving the oxido and carboxylate ligands.

One can clearly observe the effect of the oxidation of Mn^{II} (in a trinuclear complex, e.g. **1**) to Mn^{III} (in a tetranuclear complex, e.g. **4**) upon the UV absorption. The intensity of the two higher energy bands (206 and 220 nm) increased considerably as a result of additional peripheral thiocarboxylate around the Mn-centers in complex **4** which enhanced the inter- and intra-ligand charge transfers. Also, the oxidation on Mn(II) → Mn(III) shifts the lower energy bands (315 and 490 nm) gradually to longer wavelengths to be observed at 346 and 502 nm. This effect is indicative of ligand π-$d\pi$ interactions between the thiophenecarboxylate system and the metal ion, which destabilize the ligand π molecular orbitals and decrease the π–π^* energy gap, thus producing a bathochromic shift. Complex **4** shows additional absorption bands at 660 and 760 nm, assignable d → d transitions into Mn(III) ions.

The tetranuclear complexes **4**–**8** show sharp absorption bands at *ca.* 208, 224, 342 nm (UV region) attributed to $\pi \rightarrow \pi^*$ transitions and carboxylate charge transfer (LLCT). Additionally, two broad absorption bands in the lower energy region centered at *ca.* 465 and 478 nm (visible region), which are responsible for the *d*–*d* transition ($d_{xy} \rightarrow d_{x^2-y^2}$; $b_{2g} \rightarrow b^*_{1g}$), LMCT and MLCT [41], and 749 nm due to the *d*–*d* transition ($d_{z^2} \rightarrow d_{x^2-y^2}$) [41]. A characteristic signal at 320 nm for **5** could be ascribed to the $\pi \rightarrow \pi^*$ transition of the 2,2′-bipyridine ligand [20]. The replacement of thiophenecarboxylate with benzoates give rise to a slight change in the ultraviolet region bands and a derivative-type signal in the visible region, the visible feature may result from a low energy O_2CAr to metal charge transfer band, but did not affect the d → d transitions bands to a great extent which consistent with the Wells et al. work [40]. This suggests insensitivity of the intra-metal (d → d) transitions to carboxylate substitutions.

3.4. X-ray crystallography

$[Mn_3O(O_2CTh)_6(py)_3]$ (1). Plots of the molecular unit of complexes **1** from **1**·CH_3CN and **1**·~H_2O are shown in Fig. 3. Selected interatomic distances and angles are listed in Table 2. The crystal structures of **1** consist of a neutral $[Mn_3O(O_2CTh)_6(py)_3]$ complex and lattice CH_3CN or water solvent molecules. The complex unit consists of three Mn-atoms, deposited in a triangular arrangement and bridged by a central μ_3-oxido atom O(1) in the plane of the Mn-centers. The bridging $ThCO_2^-$ ligands are placed above and below the plane defined by the three Mn atoms in a pseudo-octahedral arrangement as a result of the local symmetry. The pyridine bound to the three Mn-ions at the periphery of the structure. Pyridine planes form torsion angles between 66–89° with the Mn_3 plane. Edges of the Mn_3 triangle are connected by a η^1:η^1:

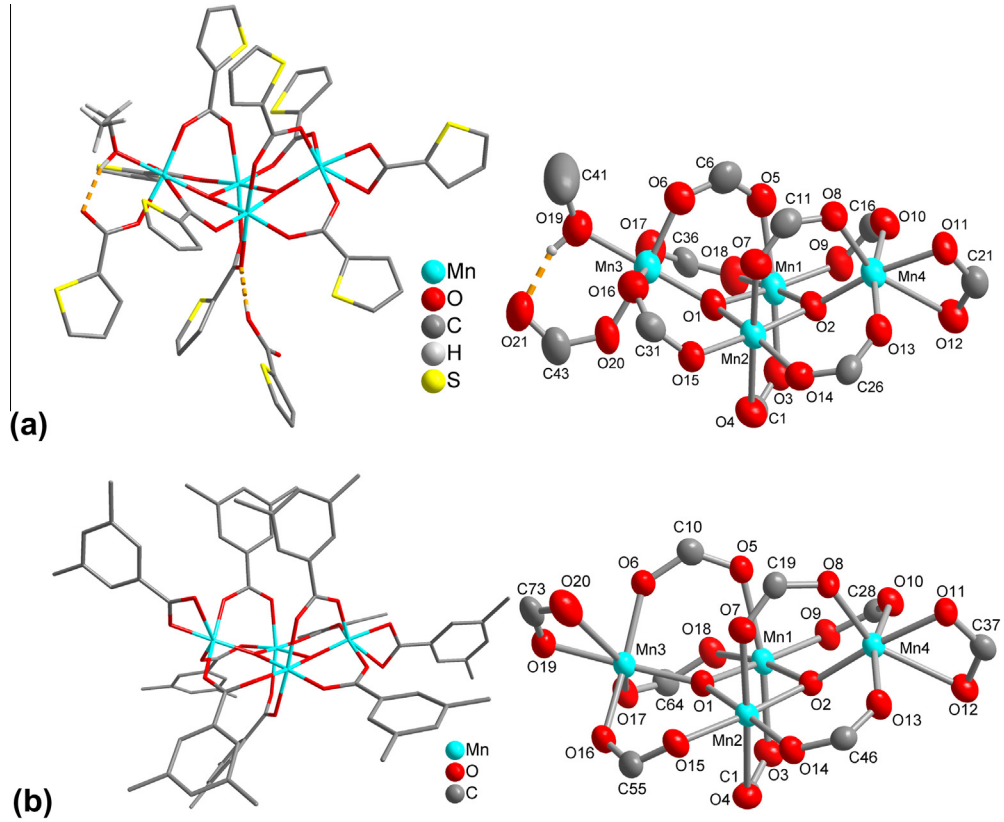

Fig. 4. Wire-frame and ellipsoid-core model (50% probability) of the anion of (a) compound **4**·$ThCO_2H$·CH_2Cl_2 and (b) compound **8**·CH_2Cl_2. H-bonds in **4**·$ThCO_2H$·CH_2Cl_2 are shown as orange dashed lines (from EtOH: H···O = 1.88 Å, O···O = 2.696(9) Å and O–H···O = 169°; from $ThCO_2H$: H···O = 1.69 Å, O···O = 2.476(10) Å and O–H···O = 158°). The counter-ion $(NBu^n_4)^+$, CH_2Cl_2 solvent, thiophene disorder and H-atoms on thiophene or dimethylphenyl ligands are omitted for clarity. Both anions employ the same atom numbering scheme for direct comparison of their bond lengths (cf. Table 4).

μ_2-$ThCO_2^-$ ions (in *syn–syn* modes) and each Mn atom occupies the center of a distorted octahedron, consisting of μ_3-O, four carboxylate oxygen and a terminal pyridine nitrogen atom to complete the coordination. The Mn···Mn separations are slightly different (Table 2) and the triangle type is approximately isosceles due to the two different Mn oxidation states. The larger Mn^{II} atom yields longer Mn-ligand bonds and thus Mn···Mn distances (cf. Table 2). The oxidation states of the three Mn-atoms were established as $Mn^{III}_2Mn^{II}$ by bond valence sum calculations [42,43] (Table 3) and inspection of Mn–O and Mn–N bond distances (cf. Table 2), so that Mn1 and Mn2 in Fig. 3 were clearly assigned as Mn(III), while Mn3 is Mn^{II} (Table 3). The Mn^{III} atoms are high-spin d^4 ions and, thus, exhibit a geometrical Jahn–Teller (JT) distortion with axial elongation, typically of ~0.1–0.2 Å for bonds along JT axes.

$(NBu^n_4)[Mn_4O_2(O_2CTh)_9(EtOH)]\cdot ThCO_2H\cdot CH_2Cl_2$ (**4**·$ThCO_2$·$H\cdot CH_2Cl_2$). X-ray structural analyses of compound **4** reveals crystallization of the cation–anion pair with a 2-thiophenecarboxylic acid and a CH_2Cl_2 solvent molecule in the asymmetric unit. Fig. 4a represents the molecular structure of the anion, and selected bond lengths and angles for **4** are given in Table 4. The anion contains the $[Mn_4(\mu_3\text{-}O)_2]^{8+}$ core with an all Mn^{III} oxidation level and "butterfly-like" arrangement. The peripheral ligation provided by nine carboxylate groups and an ethanol ligand results in six-coordinated Mn^{III} centers with distorted octahedral geometry. The $ThCO_2^-$ ligands are of two types: either bridging in the usual μ_2-manner (bidentate) between Mn ions within the butterfly unit, or in μ_1-fashion (monodentate) with one O-atom tied up as an H-bond acceptor of the EtOH group. The anion structure of **4** is very similar to that of $(NBu^n_4)[Mn_4O_2(O_2CPh)_9(H_2O)]$ (**6**). [14] The main structural features of similarity and difference of the anion of complex **4** to that of **6** are summarized as follows: (i) The anion in **4** possesses a "butterfly-like" $[Mn_4O_2]^{8+}$ core with a rhombic body skeleton (Mn_2O_2) which is analogous to **6**. (ii) The distance of the body Mn atoms $Mn_b\cdots Mn_b$ (cf. Fig. 1a) in **4** is much larger than in **6** (2.8251(16) versus 2.2155(3) Å) while the torsion angle within the rhombic backbone plane is smaller (8.84(2)° versus 11.0(5)°). (iii) Wings of the butterfly core for **4** are more extended than those of **6** ($Mn_w\cdots Mn_w$ = 5.685(3) versus 5.498(4) Å). (iv) The dihedral angle between the body plane (O1–Mn1–O2–Mn2) and wing plane (Mn3–O1–O2–Mn4) for **4** and **6** is very similar (89.2(1)° versus (89.81(1)°).

$(NBu^n_4)[Mn_4O_2(O_2CPh\text{-}3,5\text{-}Me_2)_9]\cdot CH_2Cl_2$ (8). The molecular structure of the anion of complex **8** is given in Fig. 4b; selected bond distances and angles are listed in Table 4. Complex **8** crystallizes as a cation–anion pair and a CH_2Cl_2 solvate molecule. The cation and ion lattice arrangement will not be discussed further. The anion exhibits idealized C_2 symmetry and contains the familiar $[Mn_4(\mu_3\text{-}O)_2]^{8+}$ core with an all Mn^{III} oxidation level and "butterfly-like" arrangement. The peripheral ligation provided by nine carboxylate groups giving six-coordination at each Mn^{III} center with distorted octahedral geometry. Seven carboxylate ligands bind the Mn^{III}-centers in the bridging fashion while the reaming two are chelating to a wing-Mn atoms. The "butterfly-like" arrangement is similar to that in previously reported tetranuclear manganese complexes [2–4,14]. However, the anion **8** shows two marked differences from the reported Mn_4 complexes: (i) The terminal H_2O or EtOH ligand at one wingtip position of the $[Mn_4O_2]^{8+}$ butterfly unit has been replaced by a chelating carboxylate moiety. (ii) The two Mn_w atoms are surrounded by mixed four- and six-membered chelate rings from bidentate chelating and Mn–Mn bridging carboxylate groups, respectively (Fig. 4b).

Table 2
Selected bond distances (Å) and angles (°) in **1**·CH_3CN and **1**·∼H_2O.

	1·CH_3CN	**1**·∼H_2O
Mn1–O1	2.212(4)	2.193(8)
Mn1–O3	1.969(5)	1.965(9)
Mn1–O10	1.972(4)	1.949(9)
Mn1–O12	2.126(4)	2.109(8)
Mn1–O13	1.831(4)	1.832(7)
Mn1–N1	2.076(5)	2.083(10)
Mn2–O2	2.030(5)	2.042(8)
Mn2–O4	2.106(5)	2.099(9)
Mn2–O5	2.068(5)	2.040(9)
Mn2–O7	2.032(4)	2.042(8)
Mn2–O13	1.819(4)	1.827(7)
Mn2–N2	2.103(6)	2.113(10)
Mn3–O6	2.134(5)	2.155(8)
Mn3–O8	2.156(4)	2.180(9)
Mn3–O9	2.177(5)	2.166(9)
Mn3–O11	2.134(5)	2.162(9)
Mn3–O13	2.136(4)	2.149(7)
Mn3–N3	2.270(6)	2.285(10)
Mn1–Mn2	3.2234(13)	3.225(2)
Mn1–Mn3	3.4198(13)	3.431(2)
Mn2–Mn3	3.3767(13)	3.403(2)
O13–Mn1–O3	95.44(17)	96.0(3)
O13–Mn1–O10	95.41(17)	95.3(3)
O3–Mn1–O10	168.58(18)	168.4(4)
O13–Mn1–N1	178.4(2)	179.7(4)
O3–Mn1–N1	84.89(19)	83.8(3)
O10–Mn1–N1	84.4(2)	84.9(4)
O13–Mn1–O12	95.83(16)	96.4(3)
O3–Mn1–O12	91.96(19)	91.3(4)
O10–Mn1–O12	90.48(18)	90.0(4)
N1–Mn1–O12	82.56(19)	83.8(3)
O13–Mn1–O1	96.55(17)	96.5(3)
O3–Mn1–O1	87.23(19)	87.1(4)
O10–Mn1–O1	88.00(18)	89.1(4)
N1–Mn1–O1	85.06(19)	83.3(4)
O12–Mn1–O1	167.61(17)	167.1(3)
O13–Mn2–O2	95.45(18)	95.9(3)
O13–Mn2–O7	96.24(17)	96.6(3)
O2–Mn2–O7	167.57(19)	166.9(3)
O13–Mn2–O5	96.42(18)	96.4(3)
O2–Mn2–O5	87.7(2)	88.0(4)
O7–Mn2–O5	95.12(18)	94.5(4)
O13–Mn2–N2	179.1(2)	179.5(4)
O2–Mn2–N2	84.4(2)	83.8(4)
O7–Mn2–N2	84.0(2)	83.7(4)
O5–Mn2–N2	82.7(2)	83.3(4)
O13–Mn2–O4	94.23(17)	94.8(3)
O2–Mn2–O4	89.2(2)	89.8(4)
O7–Mn2–O4	85.75(18)	85.2(4)
O5–Mn2–O4	169.15(18)	168.8(3)
N2–Mn2–O4	86.6(2)	85.6(4)
O6–Mn3–O11	172.68(19)	173.3(3)
O6–Mn3–O13	93.01(16)	92.2(3)
O11–Mn3–O13	93.93(17)	93.7(3)
O6–Mn3–O8	97.82(18)	97.4(3)
O11–Mn3–O8	84.22(19)	85.6(4)
O13–Mn3–O8	92.33(16)	91.7(3)
O6–Mn3–O9	88.91(19)	89.2(4)
O11–Mn3–O9	88.6(2)	87.4(4)
O13–Mn3–O9	91.54(16)	91.5(3)
O8–Mn3–O9	172.05(18)	172.5(4)
O6–Mn3–N3	85.41(19)	85.7(3)
O11–Mn3–N3	87.6(2)	88.5(3)
O13–Mn3–N3	178.2(2)	177.6(3)
O8–Mn3–N3	88.7(2)	87.7(4)
O9–Mn3–N3	87.7(2)	89.3(4)
Mn2–O13–Mn1	124.1(2)	123.6(4)
Mn2–O13–Mn3	117.02(19)	117.5(4)
Mn1–O13–Mn3	118.89(19)	118.9(3)

In the anions of both **4** and **8** the butterfly disposition of the Mn_4 core leads to three, distinctly different, types of Mn–Mn separations (cf. Table 4). The chelating carboxylate coordination towards one or both wing-Mn atoms results in a very distorted octahedral coordination environment for Mn4 in **4** and Mn3 and Mn4 in **8**. Directions of the Jahn–Teller distortion for the high-spin d^4-Mn^{III} ions can clearly be assigned by the trans-axial elongation of the Mn–O bond lengths by ∼0.1–0.2 Å (cf. Table 4).

Table 3
Bond valence sums *s* for Mn atoms in **1**.[a]

	s in **1**·CH_3CN Assumed oxidation state		*s* in **1**·∼H_2O Assumed oxidation state	
	+2	+3	+2	+3
Mn1	3.41	3.19	Not calculated	3.25
Mn2	3.39	3.16	Not calculated	3.14
Mn3	2.24	2.09	2.15	Not calculated

[a] Bond valences (*s*) calculated from the bond lengths (*R*) according to $s = \exp(R_0 - R)/B$ and $R_0 = 1.790$ for Mn^{2+}–O^{2-}, 1.760 for Mn^{3+}–O^{2-}, 1.862 for $Mn^{2+/3+}$–N^0, $B = 0.37$. Program VALENCE (Version 2.00, February 1993) [42].

Table 4
Selected bond distances (Å) in the anions of **4**·$ThCO_2H$·CH_2Cl_2 and **8**·CH_2Cl_2.[a]

	4·$ThCO_2H$·CH_2Cl_2	**8**·CH_2Cl_2
Mn1–O1	1.887(5)	1.849(3)
Mn1–O2	1.895(4)	1.913(2)
Mn1–O3	2.175(6)	2.177(2)
Mn1–O5	2.231(6)	2.207(2)
Mn1–O9	1.959(5)	1.906(3)
Mn1–O18	1.939(5)	1.962(2)
Mn2–O1	1.891(5)	1.850(2)
Mn2–O2	1.901(5)	1.906(2)
Mn2–O4	2.252(5)	2.208(3)
Mn2–O7	2.149(6)	2.201(3)
Mn2–O14	1.971(5)	1.915(2)
Mn2–O15	1.927(5)	1.945(3)
Mn3–O1	1.863(5)	1.826(2)
Mn3–O6	1.916(6)	1.937(2)
Mn3–O16	2.186(5)	1.955(2)
Mn3–O17	2.173(6)	2.110(3)
Mn3–O19	1.964(5)[b]	1.902(2)[d]
Mn3–O20	1.988(6)[c]	2.631(4)[d]
Mn4–O2	1.845(5)	1.823(2)
Mn4–O8	2.075(5)	1.989(3)
Mn4–O10	1.981(5)	2.026(3)
Mn4–O11	1.957(5)	1.931(2)
Mn4–O12	2.371(5)	2.363(3)
Mn4–O13	1.987(5)	2.031(2)
Mn1–Mn2	2.8251(16)	2.8090(8)
Mn1–Mn3	3.3323(17)	3.2916(8)
Mn1–Mn4	3.3952(18)	3.3792(8)
Mn2–Mn3	3.3923(18)	3.3712(8)
Mn2–Mn4	3.3175(18)	3.2920(7)
Mn3–Mn4	5.6853(24)	5.8133(9)

[a] Selected angles are given in Supplementary material in Table S3.
[b] Mn3–O19(EtOH) in **4**.
[c] Mn3–O20 to monodentate carboxylate group in **4**.
[d] Terminal bidentate carboxylate in **8**.

4. Magnetic susceptibility studies

DC magnetic susceptibility data for compounds **4**–**8** were collected in the 1.8–300 K temperature range under a field of 0.1 T (Fig. 5). The χT products of all compounds reach ∼8.5 cm^3 K/mol at room temperature, which is less than the expected value of 12.0 cm^3 K/mol for four Mn^{III} cations in compounds **4**, **6**–**8** and 13.375 cm^3 K/mol for three Mn^{III} and one Mn^{II} ion in compound **5**, respectively. All χT products show continuous decrease upon cooling in the full temperature range. From this type of thermal variation of the χT products, it is safe to conclude that this

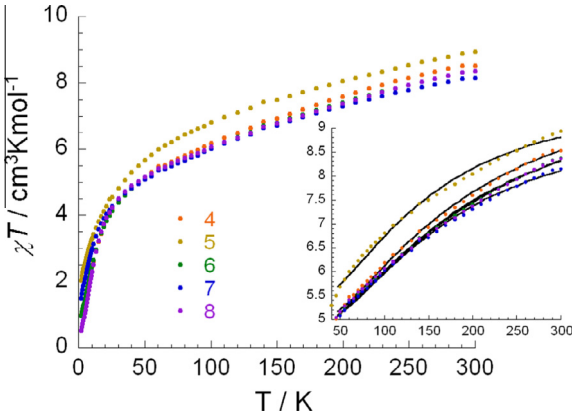

Fig. 5. Plots of χT vs. T at the applied field of 0.1 T for **4**–**8**. Inset: the solid lines represent the best fits based on the tetranuclear model for a butterfly-like core.

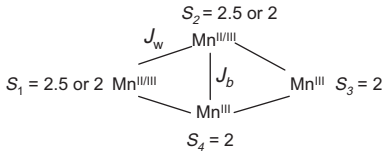

Scheme 3. Schematic representation of magnetic coupling within the butterfly core $[Mn_4(\mu_3\text{-}O)_2]$ with all Mn^{III} ions in compounds **4**, **6**–**8** and three Mn^{III} and one Mn^{II} ion in compound **5**.

behavior is associated with dominating antiferromagnetic interactions within the cluster.

To quantify the magnetic interactions between $Mn^{II/III}$ ions, a tetramer model [2,14] incorporating only two kinds of exchange pathways was considered as shown in Scheme 3. This approximation allows us to use the Kambe's vector coupling method to solve the following Hamiltonian.

$$\hat{H} = -J_w(S_T^2 - S_{13}^2 - S_{24}^2) - J_b(S_{13}^2 - S_1^2 - S_3^2)$$

where $S_{13} = S_1 + S_3$, $S_{24} = S_2 + S_4$ and $S_T = S_{13} + S_{24}$, where J_w and J_b identify the magnetic exchange coupling constant between the pairs of $Mn^{II/III}$ in the body and the wing position, respectively (cf. Fig. 1). The corresponding eigenvalues are expressed as $E(S_T) = -J_w[S_T(S_T + 1) - S_{13}(S_{13} + 1) - S_{24}(S_{24} + 1)] - J_b[S_{13}(S_{13} + 1)]$. The resulting Van Vleck equation was then used to least-squares-fit the experimental data. As shown in Fig. 5 inset, the χT products can be well fitted only in the temperature range above 50 K. The fitting parameters are summarized in Table 5. These results show a common large negative J_b and relatively smaller J_w, which are consistent with the fitting parameters published for many well-known butterfly-like Mn^{III}_4 cores [2,14]. The negative J_w and J_b values indicate dominant antiferromagnetic interactions exist between the $Mn^{II/III}$ ions. It is worthwhile pointing out that any attempt to model the magnetic susceptibility data at low temperatures failed even if we used the mean-field approach to incorporate intermolecular interactions (zJ). The possible reason for that might be that the local single-ion anisotropy of Mn(III) ions, originated from the Jahn–Teller distortion, cannot be excluded from the exchange Hamiltonian.

Table 5
Fitting parameters for compounds **4**–**8** based on a tetranuclear metallic core.

	4·$ThCO_2H{\cdot}CH_2Cl_2$	**5**[a]	**6**	**7**·$0.5CH_2Cl_2$	**8**·CH_2Cl_2
J_w (cm^{-1})	−4.60 (8)	−2.99 (8)	−4.86 (9)	−4.76 (7)	−4.89 (10)
J_b (cm^{-1})	−14.22 (47)	−12.96 (69)	−14.50 (46)	−14.24 (38)	−15.53 (52)
g	1.99 (0)	2.0 (fixed)	2.0 (fixed)	2.0 (fixed)	2.0 (fixed)
N_α ($\times 10^{-3}$) (cm^3/mol)	−1.1 (2)	−2.4 (3)	−1.9 (3)	−2.7 (0)	−1.6 (3)

[a] Similar set of parameters were obtained wherever the Mn(II) ion is located in the body or the wingtip.

5. Conclusions

We have synthesized and characterized three mixed-valence trinuclear clusters $[Mn_3O(O_2CTh)_6(L)_x(H_2O)_y]$ (**1**–**3**) containing a $[Mn^{II}Mn^{III}_2(\mu_3\text{-}O)]^{6+}$ core, four single-valence tetranuclear anionic clusters in $(NBu^n_4)[Mn_4O_2(O_2CAr)_9(L)]$ (**4**, **6**–**8**) and one mixed-valence tetranuclear complex $[Mn_4O_2(O_2CTh)_7(bpy)_2]$ (**5**). The tetranuclear complexes **4**–**8** possess a butterfly-like $[Mn_4(\mu_3\text{-}O)_2]$ core. Complexes **1**–**5** appear to be the first tri- and tetranuclear Mn complexes employing a thiophencarboxylato ligand. A similar magnetic behavior has been observed for all tetranuclear compounds **4**–**8**, in which antiferromagnetic interactions are present between pairs of manganese ions with amplitude of ~14.5 cm^{-1} and ~4.6 cm^{-1} for the body and wing, respectively. The present work demonstrated that a modification on the bridging carboxylate ligand size from Ar = –thiophene (**4**, **5**) –Ph (**6**), –Ph-*p*-Me (**7**) to –Ph-3,5-Me_2 (**8**) does neither influence the structural features nor the associated magnetic properties. Nevertheless, this ligand modification strategy presented here may provide an avenue to fine tune the magnetic properties of the magnetic clusters. The thiophene-carboxylate compounds $[Mn_3O(O_2CTh)_6(L)_x(H_2O)_y]$ and $(NBu^n_4)[Mn_4O_2(O_2CTh)_9(L)]$ are possible gold-surface binding candidates for the preparation of monolayer SMM.

Acknowledgments

This work was in part supported by DFG Grant Ja466/24-1 (initiation of bilateral cooperation RFME-CJ). Y.L. would like to thank Prof. Annie K. Powell for her generous support and also the DFG Center for Functional Nanostructures for the financial support.

Appendix A. Supplementary data

CCDC 927031–927034 contain the supplementary crystallographic data for this paper. These data can be obtained free of charge from The Cambridge Crystallographic Data Centre via http://www.ccdc.cam.ac.uk/data_request/cif. Supplementary data associated with this article can be found, in the online version, at http://dx.doi.org/10.1016/j.ica.2013.03.019.

References

[1] (a)V.L. Pecoraro (Ed.), Manganese Redox Enzymes, VCH Publishers, New York, 1992;
(b) G. Christou, Acc. Chem. Res. 22 (1989) 328.
[2] J.B. Vincent, C. Christmas, H.-R. Chang, Q. Li, P.D.W. Boyd, J.C. Huffman, D.N. Hendrickson, G. Christou, J. Am. Chem. Soc. 111 (1989) 2086.
[3] E. Libby, J.K. McCusker, E.A. Schmitt, K. Folting, D.N. Hendrickson, G. Christou, Inorg. Chem. 30 (1991) 3486.
[4] (a) E. Bouwman, M.A. Bolcar, E. Libby, J.C. Huffman, K. Folting, G. Christou, Inorg. Chem. 31 (1992) 5185;
(b) D.N. Hendrickson, G. Christou, E.A. Schmitt, E. Libby, J.S. Bashkin, S. Wang, H.L. Tsai, J.B. Vincent, P.D.W. Boyd, J.C. Huffman, K. Folting, Q. Li, W.E. Streib, J. Am. Chem. Soc. 114 (1992) 2455;
(c) S. Wang, H.-L. Tsai, K.S. Hagen, D.N. Hendrickson, G. Christou, J. Am. Chem. Soc. 116 (1994) 8376;
(d) J. Nugent, Bioenergetics 1503 (2001) 1.
[5] E.A. Schmitt, L. Noodleman, E.J. Baerends, D.N. Hendrickson, J. Am. Chem. Soc. 114 (1992) 6109.
[6] J.K. McCusker, H.G. Tang, S. Wang, G. Christou, D.N. Hendrickson, Inorg. Chem. 31 (1992) 1874.

[7] (a) J.K. McCusker, E.A. Schmitt, D.N. Hendrickson, in: D. Gatteschi, O. Kahn, J.S. Miller, F. Palacio (Eds.), Magnetic Molecular Materials, Kluwer, Boston, 1991, p. 297;
(b) D.N. Hendrickson, in: C.J. O'Connor (Ed.), Research Frontiers in Magnetochemistry, World Scientific, Singapore, 1993.
[8] (a) R. Sessoli, H.-L. Tsai, A.R. Schake, S. Wang, J.B. Vincent, K. Folting, D. Gatteschi, G. Christou, D.N. Hendrickson, J. Am. Chem. Soc. 115 (1993) 1804;
(b) R. Sessoli, D. Gatteschi, A. Caneschi, M.A. Novak, Nature 365 (1993) 141.
[9] J.R. Friedman, M.P. Sarachik, J. Tejada, R. Ziolo, Phys. Rev. Lett. 76 (1996) 3830.
[10] W. Wernsdorfer, R. Sessoli, Science 284 (1999) 133.
[11] J.B. Vincent, H.-R. Chang, K. Folting, J.C. Huffman, G. Christou, D.N. Hendrickson, J. Am. Chem. Soc. 109 (1987) 5703. and references therein.
[12] (a) H.J. Eppley, Inorg. Chim. Acta 263 (1997) 323;
(b) B. Albela, M.S. El Fallah, J. Ribas, K. Folting, G. Christou, D.N. Hendrickson, Inorg. Chem. 40 (2001) 1037;
(c) D.M. Low, E.K. Brechin, M. Helliwell, T. Mallah, E. Rivière, E.J.L. McInnes, Chem. Commun. (2003) 2330;
(d) A. Mishra, W. Wernsdorfer, K.A. Abboud, G. Christou, Inorg. Chem. 45 (2006) 10197;
(e) T.C. Stamatatos, D. Foguet-Albiol, S.-C. Lee, C.C. Stoumpos, C.P. Raptopoulou, A. Terzis, W. Wernsdorfer, S.O. Hill, S.P. Perlepes, G. Christou, J. Am. Chem. Soc. 129 (2007) 9484.
[13] (a) J.B. Vincent, H.-L. Tsai, A.G. Blackman, S. Wang, P.D.W. Boyd, K. Folting, J.C. Huffman, E.B. Lobkovsky, D.N. Hendrickson, G. Christou, J. Am. Chem. Soc. 115 (1993) 12353;
(b) L.F. Jones, G. Rajaraman, J. Brockman, M. Murugescu, E.C. Sanudo, J. Raftery, S.J. Teat, W. Wernsdorfer, G. Christou, E.K. Brechin, D. Collison, Chem. Eur. J. 10 (2004) 5180.
[14] M.W. Wemple, H.-L. Tsai, S. Wang, Inorg. Chem. 35 (1996) 6437.
[15] (a) S. Wang, H.-L. Tsai, W.E. Streib, G. Christou, D.N. Hendrickson, J. Chem. Soc., Chem. Commun. (1992) 677;
(b) S. Wang, K. Folting, W.E. Streib, E.A. Schmitt, J.K. McCusker, D.N. Hendrickson, G. Christou, Angew. Chem., Int. Ed. Engl. 30 (1991) 305.
[16] G. Christou, J.B. Vincent, Biochim. Biophys. Acta 895 (1987) 259.
[17] (a) C. Christmas, J.B. Vincent, J.C. Huffman, G. Christou, H.-R. Chang, D.N. Hendrickson, J. Chem. Soc., Chem. Commun. (1987) 1303;
(b) J.B. Vincent, J.C. Huffman, G. Christou, H.-R. Chang, D.N. Hendrickson, J. Chem. Soc., Chem. Commun. (1987) 236.
[18] (a) B. Gil-Hernández, P. Gili, J.K. Vieth, C. Janiak, J. Sanchiz, Inorg. Chem. 49 (2010) 7478;
(b) V. Marvaud, C. Decroix, A. Scuiller, C. Guyard-Duhayon, J. Vaissermann, F. Gonnet, M. Verdaguer, Chem. Eur. J. 9 (2003) 1677;
(c) J.J. Sokol, A.G. Hee, J.R. Long, J. Am. Chem. Soc. 124 (2002) 7656;
(d) H.J. Choi, J.J. Sokol, J.R. Long, Inorg. Chem. 43 (2004) 1606.
[19] (a) C. Zhang, C. Janiak, Acta Crystallogr., Sect. C 57 (2001) 719;
(b) H.H. Monfared, J. Sanchiz, Z. Kalantari, C. Janiak, Inorg. Chim. Acta 362 (2009) 3791.
[20] N. Palanisami, R. Murugave, Inorg. Chim. Acta 365 (2011) 430.
[21] T. Kuroda-Sowa, T. Nogami, M. Maekawa, M. Munakata, Mol. Cryst. Liq. Cryst. 379 (2002) 179.
[22] See for example: R.F. Mahmoud, C. Janiak, Acta Cryst. E65 (2009) m909.
[23] (a) S. Singh, J. Chaturvedi, S. Bhattacharya, Dalton Trans. 41 (2012) 424;
(b) S.J. Howell, C.S. Day, R.E. Noftle, Inorg. Chim. Acta. 360 (2007) 2669;
(c) F.A. Cotton, L.R. Falvello, A.H. Reid Jr., W.J. Roth, Acta Cryst. C46 (1990) 1815;
(d) I.A. Koval, M. Huisman, A.F. Stassen, P. Gamez, O. Roubeau, C. Belle, J.L. Pierre, E. Saint-Aman, M. Luken, B. Krebs, M. Lutz, A.L. Spek, J. Reedijk, Eur. J. Inorg. Chem. (2004) 4036.
[24] O.A. Odunola, J.A.O. Woods, K.S. Patel, Synth. React. Inorg. Met.–Org. Chem. 22 (1992) 941.
[25] B. Paluchowska, J.K. Maurin, J. Leciejewicz, J. Coord. Chem. 51 (2000) 335.
[26] T. Sala, M.V. Sargent, J. Chem. Soc., Chem. Commun. (1978) 253.
[27] APEX2, Data Collection Program for the CCD Area-Detector System, Version 2.1-0, Bruker Analytical X-ray Systems, Madison, WI, 2006.
[28] SAINT, Data Reduction and Frame Integration Program for the CCD Area-Detector System, Bruker Analytical X-ray Systems, Madison, WI, 2006.
[29] CrystalClearSM, 1.4.0. Rigaku, Coorporation, Tokyo, Japan, 2007.
[30] G.M. Sheldrick, Acta Crystallogr., Sect. A A64 (2008) 112.
[31] G.M. Sheldrick, Program SADABS, University of Göttingen, Göttingen, Germany, 1996.
[32] T. Higashi, ABSCOR, Rigaku Corporation, Tokyo, Japan, 1995.
[33] K. Brandenburg, DIAMOND (Version 3.2h), crystal and molecular structure visualization, in: K. Brandenburg, H. Putz Gbr, Crystal Impact. Bonn, Germany, 2007–2012.
[34] (a) C. Zhang, C. Janiak, Z. Anorg, Allg. Chem. 627 (2001) 1972;
(b) T.K. Maji, S. Sain, G. Mostafa, T.H. Lu, J. Ribas, M. Monfort, N.R. Chaudhuri, Inorg. Chem. 42 (2003) 709;
(c) Y.R. Martìn, M.H. Molina, F.S. Delgado, J. Pasán, C.R. Pérez, J. Sanchiz, F. Lloret, M. Julve, CrystEngComm 4 (2002) 522;
(d) V. Gómez, M. Corbella, Eur. J. Inorg. Chem. (2009) 4471.
[35] K. Nakamoto, Infrared and Raman Spectra of Inorganic and Coordination Compounds, third ed., Wiley-Interscience, New York, 1978.
[36] G.B. Deacon, R.J. Phillips, Coord. Chem. Rev. 33 (1980) 227.
[37] I. Khosravi, M. Yazdanbakhsh, J. Serb. Chem. Soc. 75 (2010) 929.
[38] J.C. Smith, E. Gonzalez-Vergara, J.B. Vincent, Inorg. Chim. Acta 255 (1997) 99.
[39] H. Visser, C.E. Dube, W.H. Armstrong, K. Sauer, V.K. Yachandra, J. Am. Chem. Soc. 124 (2002) 11008.
[40] W. Wells, A. Harton, J.B. Vincent, Biochim. Biophys. Acta 1144 (1993) 346.
[41] A.B.P. Lever, Inorganic Electronic Spectroscopy, Elsevier, Amsterdam, 1968. p. 568ff.
[42] I.D. Brown, J. Appl. Crystallogr. 29 (1996) 479.
[43] (a) I.D. Brown, R.D. Shannon, Acta Crystallogr., Sect. A 29 (1973) 266;
(b) I.D. Brown, K.K. Wu, Acta Crystallogr., Sect. B 32 (1976) 1957;
(c) I.D. Brown, D. Altermatt, Acta Crystallogr., Sect. B 41 (1985) 244;
(d) N.E. Brese, M. O'Keefe, Acta Crystallogr., Sect. B 47 (1991) 192.